Optical Non-Invasive Approaches to Diagnosis of Skin Diseases

Nikiforos Kollias and Georgios N. Stamatas
Johnson and Johnson Consumer Products Co., Skillman, New Jersey, U.S.A.

A number of noninvasive approaches have been developed over the years to provide objective evaluation of the skin both in health and in disease. The advent of computers, as well as of lasers and photonics, has made it possible to develop additional techniques that were impossible a few years ago. These approaches provide the dermatologist with sensitive tools to measure the skin's condition in terms of physiologic parameters (e.g., color, erythema and pigmentation, induration, sebaceous and stratum corneum lipids, barrier function, etc.). Yet, a typical dermatologic diagnosis relies primarily on the trained eyes of the physician and to a lesser extent on information from other senses, such as touch and smell. The trained senses of the dermatologist backed by his/her brain form a powerful set of tools for evaluating the skin. The golden rule in diagnosis remains the histologic examination of a skin biopsy, a rather invasive method. These tools have served the profession well. The advent of ever faster and cheaper computers and of sensitive, inexpensive optical instrumentation of minimal dimensions provides the professional with the possibility of making objective measures of a number of skin parameters. ***Key words: microscopy/spectroscopy/imaging/reflectance/fluorescence/Raman/confocal/Oct. JID Symposium Proceedings 7:64–75, 2002***

The human eye has a logarithmic response to light intensity and works best in contrast, e.g., an erythematous or pigmented lesion surrounded by normal skin. Instrumental measures on the other hand are capable of linear response and of absolute measurements, following calibration against a standard. In this paper we shall review some of the exciting instrumental modalities developed primarily in the last 5 y that are to a great extent bench instruments. These instruments are making the transition from bench to bedside slowly but surely and with ever increasing success. Second, we shall review some noninvasive methods of assessing optical properties of the skin and the physiologic parameters they are associated with. Finally, we shall look at a few examples of skin diseases where objective measurement techniques exist to provide measures of relevant clinical parameters.

Optical measurements are based on the interactions of nonionizing electromagnetic (EM) radiation with the skin. In the scope of this paper we will limit ourselves to radiation in the ultraviolet (UV), visible, and infrared region of the EM spectrum. An incident photon on skin may either enter the skin or be deflected at the air–skin interface due to the mismatch of the index of refraction, a phenomenon known as specular reflection. Specular reflection accounts for about 4% of the incident radiation (Hecht and Zajac, 1979; van Gemert *et al*, 1989). A photon that enters into the skin may interact with the skin's constituents in a way that will alter its direction of travel without any changes of its wavelength. This process is called scattering and occurs when EM radiation goes through an interface between two media of different indices of refraction. Some molecular species of the skin may absorb the incident EM radiation with a net result of exciting a molecule from its ground state to an excited state. The absorbed energy may be (i) dissipated as heat, (ii) re-emitted as EM radiation of lower energy (longer wavelength), or even (iii) re-emitted as radiation of higher energy (shorter wavelength), the least probable event.

The first process is absorption. The orbiting electrons of a molecule are nominally found at the lowest energy state (ground state). When an incident photon interacts with these electrons they absorb the energy and climb to an energetically higher orbit. Then the electrons may dissipate the extra energy in the form of heat and gradually return to the ground state. The wavelength of the absorbed energy is characteristic to the absorbing species and the intensity is related to its concentration. Therefore, measurements of absorption can give qualitative and quantitative information of the skin absorbers. A second possibility that an excited electron has in order to return to its ground state is to combine energy dissipation through heat with photon emission, i.e., an energy jump back to the ground state. As some of the energy of the incident photon has been dissipate to heat, the emitted photon has lower energy (longer wavelength) than the incident photon. This process is termed fluorescence. Because fluorescence involves a more complicated set of events it is less likely to occur than absorption (approximately 1000 times less frequently). The final process to consider is Raman scattering or inelastic scattering. In a Raman process EM radiation is absorbed by a molecular species at a wavelength where the molecule may have a small absorption coefficient. The molecule is excited into a state of the EM radiation field and it then decays into one of the vibrational states that make up the ground state. The difference in energy between the wavelength of the excitation photons and the wavelength of the emitted photons corresponds to the energy of the vibrational state to which the molecule has relaxed. In very rare situations the final state is energetically higher than the initial state, which corresponds to emission of a photon of shorter wavelength than the incident photon.

Manuscript received July 22, 2002; accepted for publication August 27, 2002

Reprint requests to: Nik Kollias, 199 Grandview Road, Skillman, NJ 08558

Table I. Comparison of optical technologies used in skin research and diagnostics

Technology	Emission mode	Resolution	Penetration depth
In vivo confocal microscopy	Reflectance	1 μm	<200 μm
Two-photon microscopy	Fluorescence	1 μm	0.1–1 mm
OCT microscopy	Reflectance	15 μm	1–2 mm
Raman confocal microscopy	Raman	5 μm	150 mm
Near infrared imaging	Reflectance	Depends on lens	1–3 mm
Spectral imaging	Reflectance	Depends on lens	0.1-1 mm
Three-dimensional imaging	Reflectance	1–3 μm	Only surface
Diffuse Reflectance Spectroscopy (DRS)	Reflectance	Fiber diameter	0.1–1 mm
Fluorescence Excitation Spectroscopy (FEX)	Fluorescence	Fiber diameter	0.1–1 mm
Attenuated Total Reflection-Fourier-Transformed Infrared (ATR-FTIR)	ATR	ATR crystal size	<2 μm

The above interactions of an applied EM field with molecules allow us to determine the wavelength (or energy) of different states of the molecules, which in turn allows us to determine the presence of each molecule and its concentration. Whereas absorption, scattering, and fluorescence have been studied using incoherent light sources for many years, Raman spectroscopy has only become practical with the advent of the laser. In absorption and scattering we measure approximately one-tenth to one-hundredth of the incident photons, in fluorescence we measure one-hundredth to one-thousandth of the incident photons, and in Raman scattering we measure approximately one photon for each billion photons incident on the molecules. A number of technologies have been developed into bench-top instruments in the last 5 y with a wide range of application in skin evaluation. Of these the most prominent ones are presented here (**Table I**) with two notable exceptions, the technologies of ultrasound and laser-Doppler, which have been covered extensively elsewhere (Oberg, 1990; Eun, 1995; Jemec *et al*, 2000; Ulrich and Voit, 2001; Unholzer and Korting, 2002).

BENCH-TOP TECHNOLOGIES

***In vivo* laser scanning confocal microscopy** Confocal microscopy has been developed to minimize the out-of-plane transmitted signal in the study of microscopic structures. In confocal microscopy a laser is focused onto an aperture (0.5–10 μm), which is focused in turn into the sample forming an illuminated point of equal diameter (**Fig 1**). The light from the bright spot in the sample is focused at a conjugate point through a second aperture, behind which lies the detector. The focused light is modified by the structures and chromophores it encounters in the sample. Only the light that is modified in the focal point is imaged onto the detector, however. Light that lies out of focus is excluded from the detector because it is transferred through the lens system inefficiently. Therefore, confocal microscopy allows sampling in depth with minimum interference of the overlying and underlying structures. The spot of light is scanned across the specimen at a given depth to produce an image of that optical layer. Whereas confocal microscopy of laboratory specimens is usually described in the transmittance mode, *in vivo* confocal microscopy necessitates that measurements are done in reflectance mode (Corcuff *et al*, 1993; 2001; Rajadhyaksha *et al*, 1995; 1999; Gonzalez *et al*, 1998; 1999; Huzaira *et al*, 2001). Reflectance confocal microscopes, operating with near infrared lasers (800–850 nm), have been constructed that can provide bright images of the skin to a depth of 200–250 μm. Illumination in the visible range has the drawback of limited penetration depth due to light scattering and absorption in the tissue and therefore has not been used extensively. Using illumination in the near infrared the maximum depth of imaging is limited by the scattering of the surface of the stratum corneum and the optics of the skin. Frequently, simple tape stripping of the superficial layers of the stratum corneum may be necessary to maximize penetration of the probing beam. Mucosa may be studied to greater depth (300–350 μm) due to better optical coupling. Melanin has been shown to produce excellent contrast in the study of epidermal structures (Rajadhyaksha *et al*, 1995; Corcuff *et al*, 2001). Another modality of *in vivo* confocal microscopy is fluorescence (Bussau *et al*, 1998; Vo *et al*, 1998; White *et al*, 1999). This method, however, usually requires injection of an external fluorescing marker into the skin. A number of lesions of different skin conditions have been studied *in vivo* with confocal microscopy (Gonzalez *et al*, 1998; 1999).

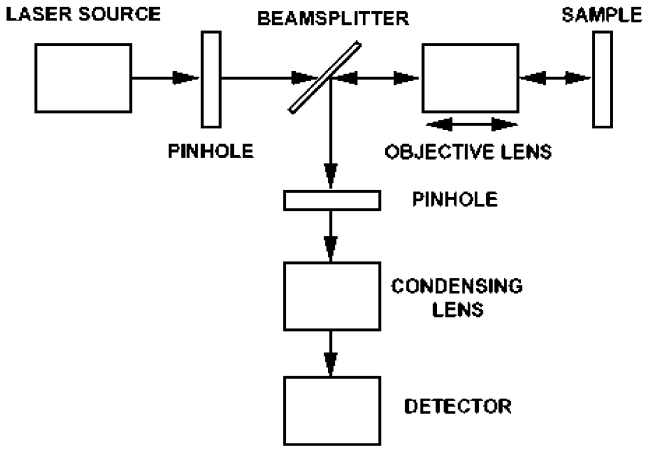

Figure 1. Schematic diagram of a confocal arrangement. Light from a laser source passes through a pinhole aperture and is focused in the sample. The point of light focus can scan the sample at different depths by means of moving the objective lens on its longitudinal axis. A second pinhole aperture is placed in a conjugate position to the first pinhole aperture in front of the detector to exclude all out-of-focus information. An image is formed at each depth within the sample by scanning the focus of the incident light in a plane parallel to the surface of the sample.

Two-photon microscopy In two-photon processes photons are compressed into a "tight" box with very small temporal and spatial dimensions (Masters *et al*, 1997a; 1997b; 1998; 1999). Under these conditions two photons may interact resulting in a photon of twice the frequency of the original photons (half their wavelength). This process may occur with three photons as well, producing a single photon of three times the frequency and a third of the wavelength. The likelihood of two-photon processes occurring is rather small (about 10^{54}); this is why the original beam has to be confined both in space and in time. In this approach the source of light is a pulsed laser with a high repetition rate (in the MHz range) and with pulses of a duration shorter than 150 fs (femtosecond $= 10^{-15}$ s). A confocal arrangement is used as above (**Fig 1**). The laser light is focused into a tight spot, which is imaged in the sample. In two-photon

microscopy near infrared photons may be used to excite in the UV fluorescing molecular species in the skin. The near infrared wavelengths propagate further into the skin because both the absorption and the scattering coefficients are minimal. Typically, laser sources exist that produce light pulses in the femtosecond range with wavelengths in the range 620–900 nm, where skin constituents absorb weakly (in two-photon microscopy irradiation in the 620–900 nm region will result in photons with 310–450 nm wavelength). The resolution obtained with this method so far is better than 1 μm laterally and 2 μm axially.

Optical coherence tomography (OCT) In OCT near infrared lasers are used to obtain a reflectance image from tissue *in vivo* (Hee *et al*, 1995; van Gemert *et al*, 1997; Welzel *et al*, 1997; Knuttel and Boehlau-Godau, 2000). The images simulate an unstained histologic section. OCT is an interferometric optical technique (**Fig 2**). The laser light is divided into two paths: in the first path light travels through air and gets reflected back by a mirror, whereas in the second path light is directed into the skin. The two reflected beams are then recombined at the detector. When the optical paths of the two beams are equal then the light from the two beams interferes constructively giving a bright spot, whereas when they are out of phase they interfere destructively. By selecting a laser with a short coherence length the interference pattern may be detected only over a short range of distances, thus making it possible to determine the depth from which the light is detected. Images are obtained by scanning the mirror at the end of the light path and by scanning the incident spot. The images are similar to an ultrasound A-scan. The resolution of OCT used to be limited to 13 μm, but has continually been improved to better than 5 μm. OCT is typically performed using optical fibers, which simplifies the adaptability of the method to *in vivo* systems (for skin as well as for internal organs accessible with optical fibers).

Raman and confocal Raman Raman spectroscopy has been applied to human skin both *ex vivo* and *in vivo* with very exciting results (Frushour and Koenig, 1975; Gniadecka *et al*, 1997; 1998; Caspers *et al*, 1998; 2001; Schallreuter *et al*, 1999; Hata *et al*, 2000; Wohlrab *et al*, 2001). The method may be implemented with optical fibers making it relatively easy to obtain information from molecular species in the skin. Several molecular species have been measured *in vivo* including keratins, β-carotene, and water, as well as exogenous materials applied to the skin. Fiber-based nonimaging systems integrate the signals from the skin often making it difficult or impossible to tell the depth from which the signals originate. This problem has been successfully overcome by combining Raman spectroscopy with confocal microscopy (**Fig 1**). Thus a Raman spectrum may be obtained from each spot within the tissue where the laser is focused and concentration profiles may be generated for various molecular species. This has been demonstrated for water, urea, urocanic acid, lactate, and various amino acids. Recently a confocal microscope has been combined with a Raman spectrometer to generate a Raman map from each point within a confocal image (Caspers *et al*, 2001).

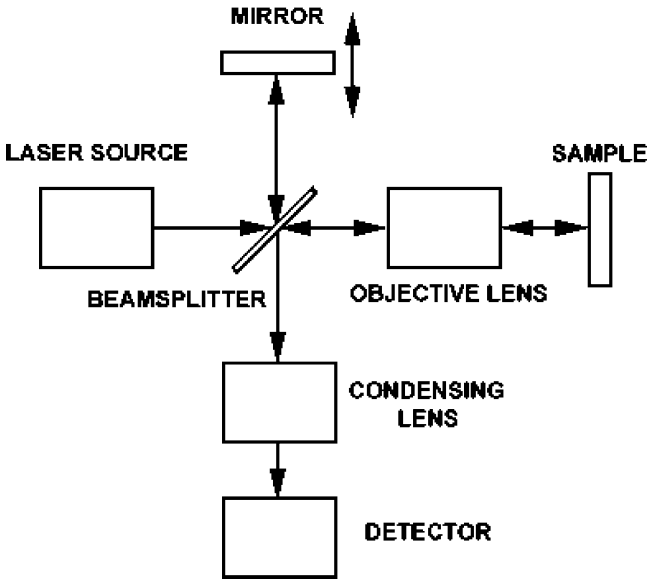

Figure 2. Schematic diagram of an interferometric arrangement for OCT. Light from the source passes through a beam-splitter. Half of the light is focused on the sample and half hits a moving mirror. The reflected light from the sample is combined with the reflected light from the mirror and the interference pattern imaged on the detector is analyzed. The depth is probed by analyzing the interference pattern as a function of the position of the moving mirror. The beam that impinges on the sample may then be scanned to obtain an image of position along the sample *versus* depth – such an image is similar to a histologic section at low resolution (≈13 mm).

Infrared imaging The development of night vision equipment sponsored by the military has resulted in important advances in the design of sensitive two-dimensional infrared sensor arrays. Infrared images may be obtained in a number of wavelength bands with good sensitivity both in the near infrared and in the mid-infrared ranges. It has been shown that infrared viewing of unstained histologic specimens may be as rich in information as viewing with visible light of hematoxylin and eosin stained sections. This has been accomplished by acquiring full spectral information at every image pixel and then performing partial least squares or multicomponent type of analysis. Structural features of histologic sections have been associated with spectral features, thus providing a sort of wavelength staining of the section. The combination of the two, visible and infrared, may provide detection enhancements that are not possible with a single stain. Furthermore, such studies may discover infrared signals characteristic of disease states that may then be used for the characterization of tissues *in vivo*. In one particular case, near infrared spectral analysis of pigmented lesions has shown a characteristic band for dysplastic nevi, which may serve in early detection of precursor lesions for melanoma (McIntosh *et al*, 1999; 2001). To date infrared spectral imaging is impractical to perform *in vivo* due to motion effects as the currently available detectors require long sampling times.

Spectral imaging This refers to a method that allows the acquisition of spectral data from every pixel in an image. The spectral resolution depends on the type of filter or wavelength dispersive element that is placed in front of the camera. In a typical arrangement a tunable filter (liquid crystal tunable filter, LCTF) is placed in front of a monochrome CCD camera (**Fig 3**). The filter is then rapidly scanned through the wavelength range of interest under computer control. The low efficiency of the currently available filters requires a bright light source that covers the wavelength range of interest. LCTFs work well in visible as well as in near infrared with a spectral resolution that becomes broader as the wavelength increases (±5 nm at 400 nm progressively increasing to ±15 nm at 1000 nm). Spectral imaging may be used to identify chromophores or molecular species through their absorption bands (Marchesini *et al*, 1995; Farkas and Becker, 2001). False color images of the distribution and concentration of each chromophore in the skin can then be generated. It should be kept in mind that the depth of tissue probed by various wavelengths is not constant but is determined by the absorption and scattering properties of the tissue. Typically, the penetration depth of light is of the order of 100 μm at the shortest wavelengths in the visible (400 nm) and 700 μm at the longest visible wavelength (700 nm). In the near infrared (700–2000 mm) radiation may penetrate to depths greater than 1 mm. In this wavelength range the penetration depth is defined by the absorption bands of water. The skin

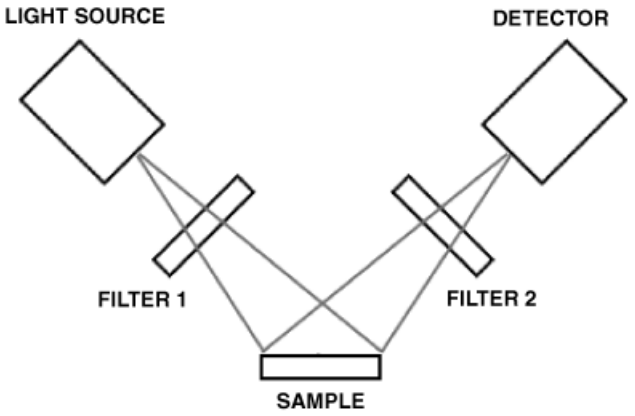

Figure 3. Schematic diagram of an imaging system using filters. Filter 1 can be a bandpass filter or a polarizer. Filter 2 can be a bandpass filter, an LCTF, or a polarizer (positioned either parallel or perpendicular to filter 1). In the case of three-dimensional imaging a fringe pattern projector is in the place of filter 1.

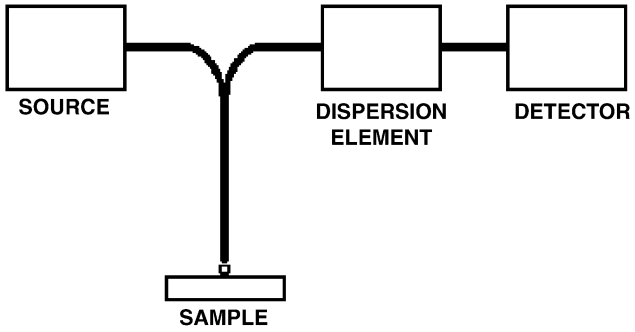

Figure 4. Schematic diagram of a diffuse reflectance spectrometer. Light illumination is delivered on the skin site of interest by means of an optical fiber bundle. Diffusely reflected light is collected by another set of fibers and is analyzed in terms of its chromatic components or constituent chromophores (color absorbing substances).

layers that are interrogated are determined by the depth to which light penetrates.

Three-dimensional imaging In the past imaging has been confined to two dimensions, i.e., images have provided little quantitative information on the three-dimensional structure of tissue. Thus raised lesions have had to be visualized by illuminating the tissue at an angle to obtain shadows, which in turn could be used to estimate height. We now have devices that allow precise determination of the volume of any raised lesion or three-dimensional structure of the skin. Three-dimensional imaging has been accomplished in a variety of ways. In a typical arrangement, a pattern of lines is projected onto the skin surface and a camera records the deviation from a straight line of the reflected light due to the variations in height of the tissue surface (**Fig 3**). A series of images of lines of ever increasing density are projected onto the skin in order to determine both the gross contours (e.g., of the face) as well as the fine structure (e.g., pores). The images are converted to height information of each surface point with a computer. The height information may then be visualized with the aid of additional software by viewing from different angles, i.e., simulating what happens in real life when we want to perceive depth accurately. These devices have been extensively used for the determination of the length and volume of wrinkles and of facial contours.

These technologies represent only a sample of the most prominent ones currently in use in skin research. The instruments are "bench" type, meaning that the subject has to go to the instrument rather than the other way around. The other consideration is cost of purchase as well as cost of operation. Cost of purchase ranges from US$50,000 to US$150,000 and some of these require the presence of a scientist for the interpretation of the data, as well as for the operation of the instrumentation. Of these the ones that have been implemented in clinical settings are the laser scanning confocal microscope (US$80,000–100,000), OCT (which has been independently developed in many laboratories) (US$50,000–80,000), and three-dimensional imaging (US$10,000–40,000).

SINGLE POINT MEASUREMENTS

The most commonly used instrumentation to date to evaluate the properties of skin involves single point measurements and photography. Typically in single point methodologies, several measurements are acquired over a region of interest; they are averaged and then referenced to some standard (absolute measurements) or compared to adjacent uninvolved ("normal") skin. The first approach allows measurements of specific skin parameters, such as conductivity, color, elasticity, etc. The second approach takes into account biologic variability and gives an apparent added sensitivity. Average values over populations tend to carry large uncertainties, whereas variations of particular parameters for a single individual may remain fairly constant over time. Furthermore, skin measurements may be classified in two groups: those that relate to skin properties at a fixed point in time (static) and those that assess the responses of skin over time to various stimuli (dynamic).

Measurement of specific physical-chemical properties of the skin allows the determination of skin parameters, such as electrical (conductivity, pH, etc.), mechanical (elasticity, plasticity, etc.), acoustical (propagation of sound), optical (absorption, scattering, etc.), structural (surface geometry, volume, etc.), thermal (heat loss, etc.), chemical (permeability, composition, etc.), and others. In this report we shall concentrate on the optical properties. We can obtain information on a number of parameters from single spectral measurements. For example, a measurement of the reflectance spectrum of the skin in the visible (400–700 nm), which requires approximately 0.050 s to obtain, may be analyzed for color parameters as well as for the content of the molecular species of oxyhemoglobin and deoxyhemoglobin, melanin, water, and scattering. We shall discuss the information that may be obtained from diffuse reflectance spectroscopy (DRS) in the visible, fluorescence excitation spectroscopy (FEX) in the UV and visible, and attenuated total reflection Fourier transformed infrared (ATR-FTIR) spectroscopy. All of these techniques make use of optical fiber probes and therefore measurements may be made on any part of the body. Furthermore, the DRS instrument is portable and the FEX and the FTIR instruments may be easily transported to the human subject or patient.

Spectral measurements not only allow the determination of apparent concentrations of known chromophores, but may also provide us with insights that come with detailed analysis of the spectra. For example, the roles of oxyhemoglobin and deoxyhemoglobin provide information not simply on the oxygen saturation of the tissue but also on the involvement of specific vascular plexi that may be responsible for the skin reactions. Similarly, we can find a number of distinct spectral expressions for epidermal melanin pigmentation.

DRS In diffuse reflectance light is delivered onto the skin and the reflected light is collected and analyzed with a spectrometer (**Fig 4**). Such instruments were first built and measurements were carried out more than 50 y ago (Edwards and Duntley, 1939). The instrumentation for DRS has been reduced to a handheld spectrometer, a 3 W light source, and a handheld

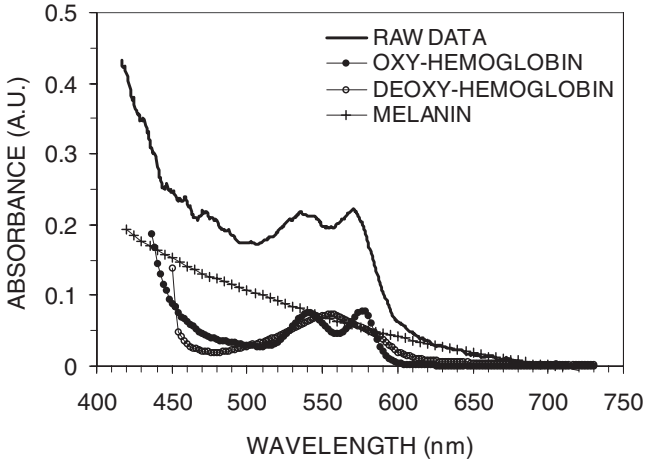

Figure 5. Typical DRS spectrum of an erythematous lesion. Spectral data were obtained with a diffuse reflectance spectrometer from a skin site with a slight erythema normalized to a white standard. The spectrum is decomposed into its component spectra of oxyhemoglobin, deoxyhemoglobin, and melanin. Concentrations of each substance may be estimated from the individual contribution.

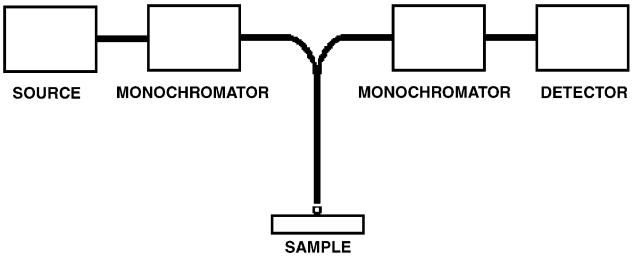

Figure 6. Schematic diagram of a fluorescence spectrometer. Light is delivered and collected from the skin site of interest with an optical fiber bundle. Double monochromators at the illumination and at the detection end allow for sensitive narrow-band excitation and emission. The monochromators can be controlled to sequentially scan the excitation or the emission or both synchronously.

computer. Light is brought to the skin and reflected light is collected by flexible optical fiber bundles. The spectra obtained from skin have features that correspond to absorption maxima of hemoglobin and of epidermal melanin pigmentation (**Fig 5**, **Table II**). The spectra may be fitted accurately using (i) a diffusion approximation model to describe the photon paths in the tissue and (ii) the absorption spectra of pure compounds. Spectral analysis provides a unique set of concentrations for the contributing chromophores (Kollias and Baqer, 1986; 1988; Andersen and Bjerring, 1990; Zonios *et al*, 2001). The results are given as apparent concentrations for each chromophore (i.e., the absorbing molecular species). The species that are necessary in order to obtain good fits include oxyhemoglobin, deoxyhemoglobin, melanin, scattering (density and size of scatterers), as well as water (Anderson and Parrish, 1981; Wan *et al*, 1981; Farrell *et al*, 1992; Kollias *et al*, 1994; 1995; 2001). Scattering is the cause for the remittance of light from the skin. On average light is scattered into an angle of 10° away from the direction of the incident beam at each scattering event. At least 324 scattering events need to take place before a photon re-emerges from the skin. This means that it traverses a long path in tissue and makes absorption events likely. Oxyhemoglobin has been found to describe well the early reactions in UV-induced erythema and chemical-induced irritation. Deoxyhemoglobin has proved to be a good marker for vascular stasis in superficial venules. Melanin has proved to be a reliable measure for constitutive pigmentation. Although the molecular species responsible for skin color may be easily characterized by their absorption maxima and detailed spectra, the trained eye may not distinguish when two chromophores coexist. When melanin pigmentation and hemoglobin responses overlap the eye has trouble in distinguishing each element's contribution. Similarly, it is hard to visually quantitate the balance between oxyhemoglobin and deoxyhemoglobin. The only way to separate the contributions is by diascopy, i.e., by compressing the skin, thus emptying the vessels of blood for a short time and allowing to realize the contribution of melanin pigmentation. Furthermore, the contributions are very difficult to separate out when the pigment reaction is not confined to a small region with well-defined borders.

Human pigmentation has been assessed histologically with the specialized stain Fontana–Mason. In investigations in which the goal was to characterize the spectral signature of induced (facultative) pigmentation, it was surprisingly determined that the spectral characteristics of facultative pigmentation depended on the stimulus (Kollias, 1992; Kollias and Baqer, 1984; 1987; Vitkin *et al*, 1994; Young, 1997). Whereas constitutive epidermal pigmentation has a spectral signature that closely resembles that of synthetic and extracted melanin, the spectral signatures of UV radiation or visible light induced epidermal pigmentation are distinct from constitutive pigmentation. UVB-induced pigmentation forms as the inflammatory process subsides following exposure (erythema) and has a spectral signature that is close to that of constitutive melanin pigmentation. The spectra of UVB-induced pigmentation differ from those of constitutive pigmentation at wavelengths shorter than 335 nm. Some of this difference may be due to the thickening of the stratum corneum. UVA-induced pigmentation has a spectral signature that is different from that of constitutive pigmentation even in the visible part of the spectrum. The UVA-induced pigment has a gray appearance immediately after exposure and changes to a brown appearance after 20 min to 1 h with a brown color that is deficient in blue – this has been confirmed with measurements with a color measuring device (chromameter). The spectrum of UVA-induced pigmentation is similar to native pigmentation at wavelengths longer than 550 nm, i.e., it decreases with wavelength at longer wavelengths. At wavelengths shorter than 500 nm instead of increasing in absorbance to shorter wavelengths it decreases down to about 340 nm. This is a characteristic feature, a *sine qua non*, of UVA-induced pigmentation. The spectral signature of UVA-induced

Table II. Absorption maxima in the visible and NIR of the principal absorbing molecular species in skin

Molecular source	Absorption max (nm)	Physiologic parameter
Oxyhemoglobin	412, 542, 577	Capillary and arteriolar blood
Deoxyhemoglobin	430, 555, 753	Venous blood
Epidermal melanin pigment	No maximum[a]	Melanin pigment
Water	760, also near infrared bands	Edema, extracellular water
Scattering	No maximum[b]	Collagen structure, edema

[a]Decreases monotonically to longer wavelengths.
[b]Decreases monotonically slowly to longer wavelengths.

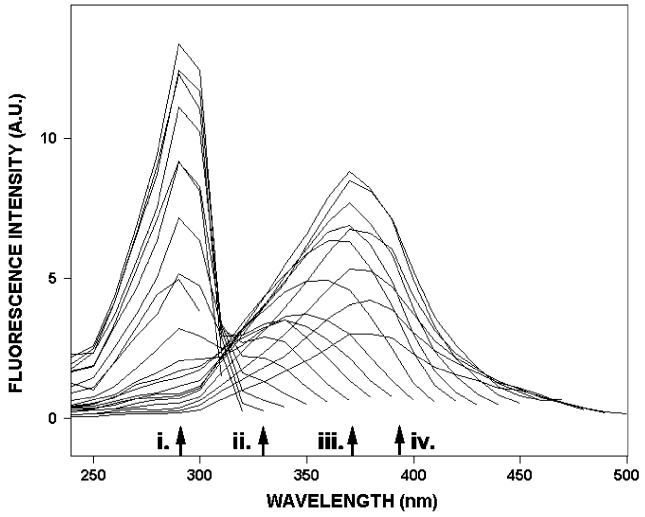

Figure 7. Typical fluorescence excitation spectra obtained from human skin. The spectral curves were produced by scanning the excitation monochromator from 240 nm to within 20 nm of the position of the emission monochromator (e.g., the first curve is produced by scanning the excitation monochromator from 240 nm to 300 nm with the emission monochromator set at 320 nm, the second by scanning the excitation from 240 nm to 320 nm with the emission set at 340 nm, and so on). The principal components of the spectra are indicated below the set of curves and correspond to (*i*) tryptophan, (*ii*) pepsin digestible collagen cross-links, (*iii*) collagenase digestible collagen cross-links, and (*iv*) elastin cross-links.

pigmentation eventually reverts back to a spectrum resembling that of melanin with time ranging from 2 h to a week depending on the individual. It is known that visible light (400–700 nm) may produce a pigment response in human skin when sufficient doses are delivered. Visible-light-induced pigmentation has been shown to have a transient component (that lasts for less than half an hour) as well as a persistent component (that may last for months). The spectral signature of this pigment is a smooth curve that increases with increasing wavelength, a behavior that is exactly the opposite of the behavior of the absorption of constitutive melanin pigmentation. Finally, psoralen plus UVA (PUVA) induced pigmentation has a spectral signature that is similar to the signature of constitutive melanin pigmentation with the addition of hemoglobin. Even following a single exposure we find an increased vascular response in all PUVA-treated sites that lasts for months.

Thus, using DRS we may not only determine the apparent concentration of absorbing molecular species in the superficial layers of the skin, but we may also characterize the reactions of the skin beyond the capabilities and power of discrimination of the human eye.

FEX *In vivo* fluorescence spectroscopy of skin (**Fig 6**) has been extensively used by many research groups (Leffell *et al*, 1988; Lohmann and Paul, 1988; Lohmann *et al*, 1994; Zeng *et al*, 1995; 1998; Richards-Kortum and Sevick-Muraca, 1996; Kollias *et al*, 1997; 1998; Bissonnette *et al*, 1998; Brancaleon *et al*, 1999; 2001b; Gillies *et al*, 2000; Gonzalez *et al*, 2000; Doukas *et al*, 2001; Na *et al*, 2001; Tian *et al*, 2001; Vo *et al*, 2001). Fluorescence measurements are usually carried out in the emission mode, i.e., radiation of a single wavelength is shone onto the skin and the emitted radiation (at wavelengths longer than the excitation wavelength) is analyzed. The question addressed is where does the skin emit radiation when excited with radiation of a certain wavelength. In FEX the emission wavelength is fixed and the excitation wavelengths are scanned; these wavelengths are shorter than the emission wavelength (**Fig 7**). The question addressed in FEX is where does the skin absorb in order to emit fluorescence at a certain wavelength. In the case of skin the excitation spectra tend to be narrower (and therefore more easily separated) than the emission spectra. Use of optical fibers allows the fluorescence of any part of the skin to be measured. The fiber bundle is bifurcated, the fibers at the joined end are randomly mixed, and this end is brought in contact with the skin. The excitation light source may be a xenon arc or a laser source. One of the legs brings radiation (light) from the excitation monochromator (the instrument that selects the wavelength of excitation) to the skin and the other leg collects light emitted by the skin and delivers it to the emission monochromator (analyzer), where emission wavelengths are selected. The light intensity is typically measured with a photomultiplier detector. It is important when doing excitation spectroscopy from the skin to use a double monochromator at the excitation. The reason is that at short wavelengths (shorter than 300 nm) the light produced by a xenon arc lamp is very weak compared with the emission at longer wavelengths (greater than 300 nm), which results in a large and sloped background if a double monochromator is not used. The instrument we have used employs a double monochromator both at the excitation and at the emission sides (SkinSkan, JY Horiba, Edison, NJ). It should be kept in mind that, although this method of acquiring measurements is simple, the signals we obtain are controlled by the optics of human skin. This means that the depth probed depends on the absorption and scattering properties of the skin at the wavelength of interest. At the short wavelengths of the UV (shorter than 300 nm) the optics of the skin are dominated by the absorption by proteins. At wavelengths longer than 335 nm the optical properties are dominated by the absorption of epidermal melanin pigmentation. The absorption maxima of hemoglobin are given in **Table II**; hemoglobin plays an important role as absorbing species limiting the penetration of light at these wavelengths.

The important fluorescence bands of molecular species in the skin are summarized in **Table III**. It is interesting to note that the excitation spectra have an isoemissive point at about 315 nm found in both human and animal skin (hairless mouse, hairless rat). It has been determined that the fluorescence excitation maxima with wavelengths shorter than 315 nm are of epidermal origin, whereas the fluorescence signals longer than 315 nm are of dermal origin. Epidermal keratins fluoresce very weakly in the skin when hydrated and fluoresce rather strongly when

Table III. The principal sources of fluorescence from human skin

Molecular source	Excitation max (nm)	Emission max (nm)	Physiologic parameter
Tryptophan	295	345	Proliferation, aging
Pepsin digestible collagen cross-links	335	380	Collagen cross-links, aging, glycation
Collagenase digestible collagen cross-links	370	420	Collagen cross-links, glycation
Elastin cross-links	400	500	Elastin cross-links
Tyrosine (?)	275	340	Inflammatory infiltrate
Coproporphyrin	405	620	*P. acnes*
"Horn"	365	430	Noninflammatory acne
NADH	350	450	Mitochondrial activity

Table IV. The principal absorbing species in skin in the mid-infrared

Molecular source	Absorption max (cm^{-1})	Physiologic parameter
Water (OH)	3420 (broad), 1640	Stratum corneum hydration
Proteins [amide I, II]	1645, 1545	Stratum corneum proteins
Lipids [CH_3] , [CH_2]	[2960, 2870] , [2920, 2850]	Stratum corneum lipids
Free fatty acids [C = O]	1710	Sebaceous lipids
Triglycerides	1740, 1460	Sebaceous lipids
Wax esters	1740	Sebaceous lipids

dehydrated, e.g., dry skin flakes and psoriatic plaques fluoresce strongly with excitation and emission maxima similar to those of "horn". The tryptophan fluorescence has been found to increase with proliferation induced by a number of agents, e.g., aging, tape stripping, retinoids, psoriasis, α-hydroxy acids, nonmelanoma skin cancer, and others. The fluorescence of pepsin digestible collagen cross-links is related to aging in both human and animal data. The fluorescence of collagenase digestible collagen cross-links appears to be insensitive in the range of parameters tested, but is sensitive to the dissolution of collagen cross-links induced by nonmelanoma skin cancer (Brancaleon *et al*, 2001a). The fluorescence of elastin cross-links increases with aging. Tyrosine fluorescence has been found in skin that has been chronically exposed to UVB radiation at close to erythema levels, in psoriatic lesions, in skin treated with 8% glycolic acid (but not in skin treated with 8% lactic acid), and in skin treated chronically with retinoids.

Thus, FEX has been found to provide objective measures on a number of important physiologic parameters in skin. More work needs to be done in order to tie down the exact correlation between fluorescing species and molecular components. A number of studies are under way.

ATR-FTIR spectroscopy There have been several reports of the use of ATR-FTIR *in vivo* on skin (Bommannan *et al*, 1990; Mak *et al*, 1990; Lucassen *et al*, 1998; Pouliot *et al*, 1999; Brancaleon *et al*, 2000; 2001b). This method constitutes an extension of DRS to the mid-infrared region of the spectrum (2–25 μm or 500–4000 wavenumbers). The mid-infrared provides information on the vibrational states of the molecular species probed. In particular, we can study the vibration of groups of atoms (such as methyl, ethyl, carboxyl, etc.) about specific bonds within the molecule. It makes it possible to study the relationship between molecular order and biologic activity. This type of measurement correlates spectral positions, spectral shifts, and intensity ratios with molecular composition and conformational order of molecules. The major bands in the mid-infrared that have been identified on skin are shown in **Table IV**. The infrared spectrum from a tissue is dominated by the absorption of water, making it difficult to obtain information about other molecular species. We can minimize the contribution of water by sampling only the superficial layers of the stratum corneum. This has been accomplished by attenuated total reflection (ATR), where infrared radiation propagates in a crystal and probes the molecules that are brought in contact with the crystal (**Fig 8**). In this case the contact between the spectrometer and the skin is effected with a ZnSe crystal, which has the shape of a cylinder of 3 mm in diameter with a tip made of a right circular cone (angle of the apex 90°). The crystal sits on the joined end of an infrared transmitting fiber optic bundle. In this geometry infrared light is directed into the crystal and then reflects from the apex twice before returning to the analyzer. At the point of reflection of light there is an evanescent field that extends beyond the surface of the crystal by approximately a quarter to a half of the wavelength of light. This field may couple to whatever agents are brought in contact with the crystal tip, in our case with skin. As absorption coefficients (extinction coefficients) in the infrared are rather large the path followed by the evanescent wave is enough to give a significant attenuation to the transmitted signal and therefore the absorption of the sample may be estimated. With this particular geometry we may study the top 1–2 μm of the skin, i.e., the surface of the stratum corneum, and obtain good and reliable measures of surface lipids and water, whether of sebaceous origin or of stratum corneum origin. A typical spectrum acquired from human skin is shown in **Fig 9**. Furthermore, it has been shown that we may distinguish between free fatty acids, triglycerides, and wax esters. We can also quantify surface water, which has been validated with measurements using other methods. Moreover, we can follow changes in these parameters over time or after treatment, as the probe is small and interferes minimally with application.

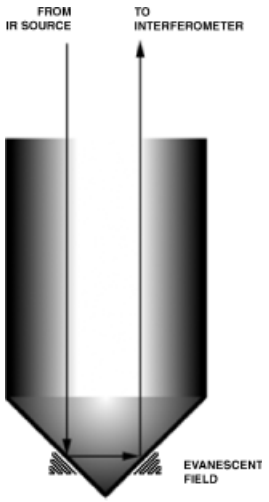

Figure 8. Schematic diagram of an ATR crystal. The tip of the crystal (approximately 2 mm in diameter) is brought into contact with the skin sample. Light from an infrared source bounces twice at the walls of the conical tip of the probe. At each bounce an evanescent field extends beyond the crystal surface into the sample at a distance of approximately a quarter to a half the wavelength of the incident light. The reflected light creates an interference pattern with part of the illumination light in a similar configuration to **Fig 2**.

Imaging Imaging may be thought of as an extension of single point measurements into two dimensions. In imaging we attempt to document what the physician perceives when he/she observes a skin lesion. An image is a two-dimensional structure and cannot possibly provide a record of what the physician perceives in its totality. The physician possesses binocular vision, which gives him/her the ability to "see" three-dimensional features as shape and structure. The physician can also observe a lesion from different angles to eliminate glare and to maximize contrast (e.g., pigmented lesions when viewed at a shallow angle present higher contrast than when viewed perpendicular to the surface of the skin). Most importantly the physician is backed by a powerful computer, his/her mind, that contains a large library of images for classification of the new observation. Therefore, a number of specialized imaging scenarios have been developed to make allowance for the shortcomings of regular photography

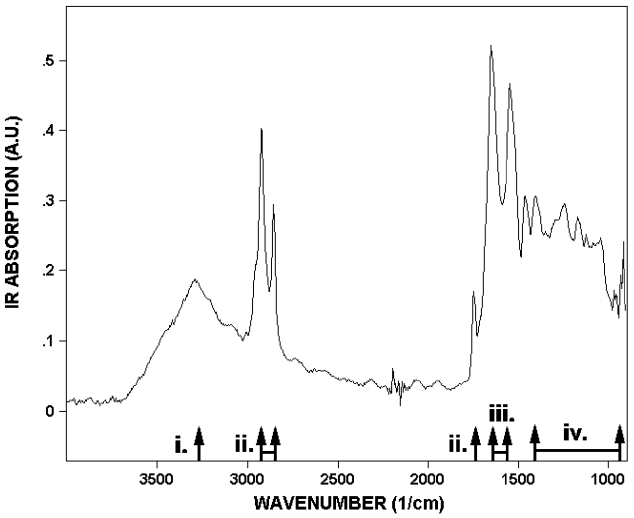

Figure 9. Typical ATR-FTIR spectrum obtained from human skin. The ATR probe was placed in contact with the skin site of interest and the FTIR spectrum was acquired. The principal components contributing to the spectrum are (*i*) water, (*ii*) lipids, (*iii*) proteins. Region (*iv*) contains information from proteins, lipids, DNA, and water and is termed the "fingerprint spectral region".

in documenting all the relevant features of a skin lesion (**Table V**). Standard photography has experienced changes with the introduction of digital cameras. It is now possible to overcome many of the problems of film, such as the variations due to production differences batch to batch and the variations in chemistry during processing, which result in variations in color quality. Digital photography can overcome these problems by calibration of the camera and color correction for intercamera variabilities and flash variabilities. Specialized techniques, such as polarized light photography and fluorescence photography (Mustakallio and Korhonen, 1966; Anderson, 1991; Muccini *et al*, 1995; Lucchina *et al*, 1996; Fulton, 1997; Kollias *et al*, 1997; Pagnoni *et al*, 1999), have been introduced to aid in documenting specific features. In polarized light photography (**Fig 10**) linear polarizing filters are used both on the camera lens and on the flash in order to selectively enhance surface features (such as fine lines and wrinkles, scale, pores, scars, raised lesions) or subsurface features (such as erythema, pigmentation, hair follicles). This is accomplished by rotating one of the filters so that its polarization orientation is either parallel or perpendicular to the orientation of the other filter. In fluorescence photography the flash is filtered to emit radiation in the long UVA (360–400 nm) and the camera is filtered to receive only radiation that is emitted by the skin (440–700 nm). Fluorescence photography has been used to enhance the distribution of pigmentation, especially solar lentigenes, *Propionibacterium acnes* and open comedones. Briefly, to document pigmentation the incident radiation excites the collagen matrix, which emits in the visible (440–600 nm). Epidermal melanin pigmentation attenuates the intensity of both the incident (more strongly) and the emitted light. Because melanin absorbs strongly in the UV region of the spectrum and in the blue a significant

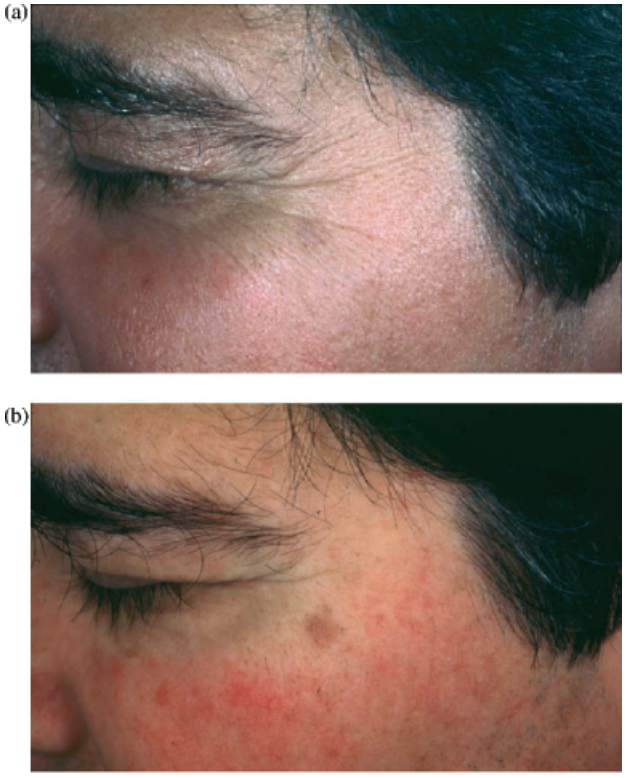

Figure 10. Images obtained under polarized light illumination. (*a*) The analyzing polarizing filter was parallel to the illumination polarization filter; (*b*) the analyzing polarizing filter was positioned perpendicular to the illumination polarizing filter. In the images shown (*a*) the surface features of the skin become selectively enhanced and (*b*) the surface features of the skin are eliminated making possible the documentation of subsurface features such as erythema and pigmentation.

enhancement is obtained in the distribution of pigmentation due to better contrast. There is no glare in fluorescence photography because the incident radiation that is reflected by the surface of the stratum corneum is filtered out of the camera by the camera filter. In the case of *P. acnes* the incident radiation excites the fluorescence of coproporphyrin that is produced by the bacterium. In the case of open comedones, the incident radiation excites the impacted or extruding "horn" in the "blackheads".

APPLICATION OF NONINVASIVE MEASUREMENTS TO DISEASE EXPRESSION OR RESPONSE TO TREATMENT

For this discussion we have selected three skin conditions on which data have been generated; these are acne, psoriasis, and nonmelanoma skin cancer.

Acne The parameters that have been assessed objectively in acne include:

Table V. Imaging modalities for documentation of skin status

Imaging modality	Instrumentation	Feature enhancement
Standard flash photography	Camera, flash, film/digital	Record of overall appearance
Polarized light photography	Include polarizing filters on camera and flash	Separation of surface from subsurface skin features, e.g., fine lines and wrinkles *versus* erythema and pigmentation
Fluorescence photography	Dark room; filters on flash and camera	"Horn" in noninflammatory acne, pigmentation, scale
Video microscopy	Video camera (handheld), light source (fiber)	Magnified view of skin surface or subsurface; magnification range 2–1000

Discrimination between inflammatory and noninflammatory acne lesions
Area of involvement for erythema
Lesions count
Extent of *P. acnes* involvement
Quantification of erythema and scale
Post-inflammatory hyperpigmentation
Scars

The method of assessment for inflammatory lesions is polarized light photography with the polarizing filters oriented perpendicularly to each other (Phillips *et al*, 1997). In this arrangement only the subsurface features are visualized, i.e., the intensity and extent of erythema and post-inflammatory hyperpigmentation. Once the image is obtained the area of involvement may be measured by image analysis software or even better by selecting the G (green) channel of the RGB (red –green – blue) image obtained by the CCD camera chip. In the green channel image, which is a gray-scale image, erythema appears black and normal skin white. The extent of scale on the other hand may be assessed from the image obtained with the polarizing filters oriented parallel to each other. In this arrangement surface features are enhanced giving the scale a white appearance. The area of involvement may then be calculated by image analysis software. Noninflammatory acne lesions may be highlighted by using fluorescence photography with an excitation in the UVA range (350–380 nm) (Lucchina *et al*, 1996). The camera lens should be filtered so that it accepts only visible radiation. An example of fluorescence, cross-polarized, and parallel-polarized imaging of acne lesions is shown in **Fig 11**. The fluorescence image obtained thus includes both the punctate (point sources) and diffuse fluorescence of coproporphyrin produced by the bacteria with a maximum emission at 620 nm (appearing red) and the punctate fluorescence of the lesions with impacted "horn", which fluoresce throughout the visible with a white appearance. Both of these sources of fluorescence always appear on a background of diffuse blue-green fluorescence due to the emission by the dermal collagen cross-links. The lesions with punctate fluorescence correspond to open comedones and may be counted, by image analysis software, to yield a lesion count. The count of coproporphyrin lesions is more indicative of pores with *P. acnes* involvement than of the severity of the disease. Such sources of fluorescence may be counted from the image using image analysis software. When a subject is treated with antibiotics or with benzoyl peroxide, the coproporphyrin fluorescence decreases all the way to zero and this signal may thus be used to assess subject compliance. The background collagen cross-link fluorescence may be used to assess scars, as the fluorescence of scar tissue differs from that of normal dermis. Care has to be exercised, because typically the fluorescence of scar-associated collagen cross-links is weaker than that of the surrounding normal collagen and will appear as a dark area on the fluorescence image, but so will inflammatory lesions. The way around this problem is to compare an image obtained with polarized light with the fluorescence image.

The intensity of erythema and induration have been assessed using single point measurements with DRS, where the spectrum obtained has been analyzed for oxyhemoglobin, deoxyhemoglobin, and dermal scattering. The signal due to dermal scattering has been shown to be a reliable measure of clinical induration. The calculated apparent concentration of oxyhemoglobin corresponds to the "redness" of the lesion and may be used as a measure of the effectiveness of treatment on selected lesions between patient visits.

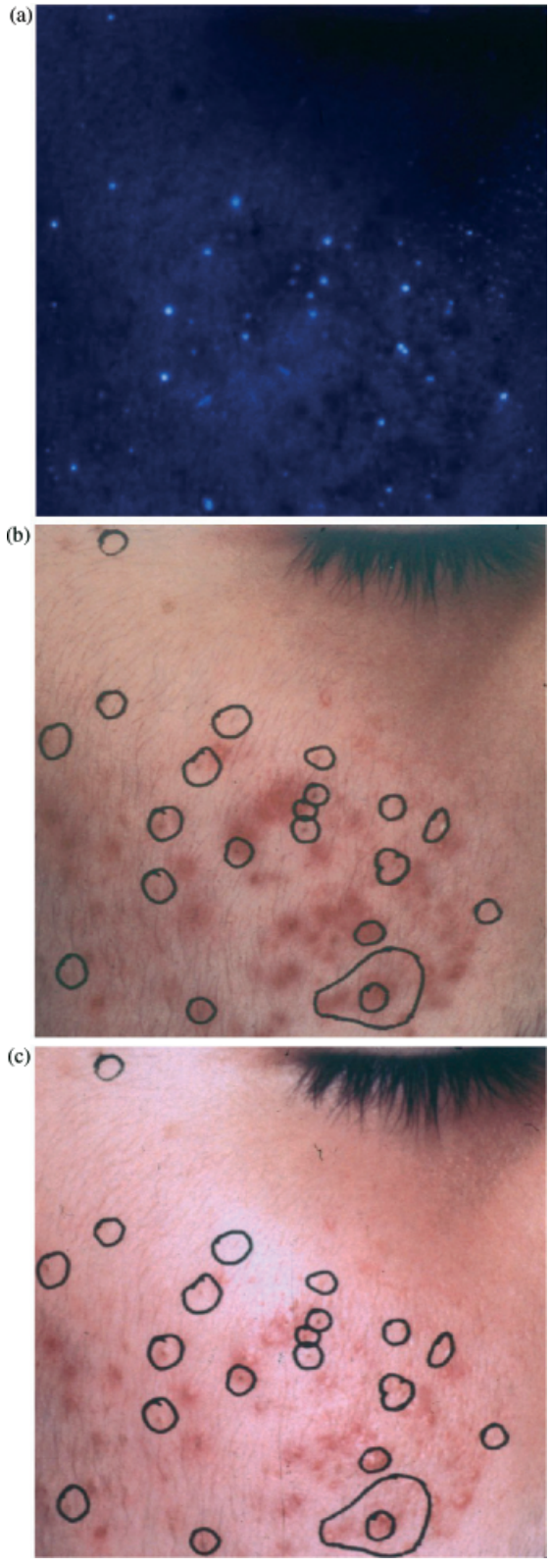

Figure 11. Images obtained from the skin of an acne subject. (*a*) A fluorescence image excited with blue light (400 nm ± 10 nm). (*b*) Reflectance image with polarized illumination and perpendicular orientation of the analyzing polarizer – the surface features of the skin are absent from the image. (*c*) Reflectance image under camera flash illumination –both the surface of the skin and some subsurface features are seen. In image (*a*) the fluorescence emission of open comedones (noninflammatory lesions) is clearly delineated. In image (*b*) the inflammatory lesions are selectively shown in the absence of surface glare –the marks correspond to the locations of the noninflammatory lesions. In image (*c*) the marks show the noninflammatory lesions and the enhancement of the inflammatory lesions of image (*b*) is partially lost, making it difficult to count lesions or the extent of the inflammatory lesions.

Psoriasis In the case of psoriasis the parameters that may be assessed objectively include:

Proliferation of keratinocytes
Epidermal inflammation
Erythema
Induration
Scale
Blood vessel morphology
Keratinocyte morphology

The extent of the disease may be assessed by polarized light photography as in the case of acne above. Cross-polarized images provide a good record of the extent of erythema by eliminating the appearance of scale. For automatic analysis of the extent of the disease the intensity attenuation due to body curvature has to be corrected for (Tanaka *et al*, 2000). This may be accomplished by intentionally blurring the image by averaging the intensity of pixels to such an extent that the resulting image has no recognizable features except for contours. The negative of this image may then be added to the original image to minimize the intensity variation due to contours. The extent of the disease may then be calculated with image analysis software from the calculated image because variations in intensity are now due only to the presence of psoriatic plaques (Savolainen *et al*, 1997). The intensity of erythema and the severity of induration may be objectively assessed with DRS and have been shown to provide a sensitive measure of the progression of the disease as well as the effectiveness of treatment (Kollias *et al*, 1994; Gonzalez *et al*, 1996).

Proliferation of keratinocytes and epidermal inflammatory infiltrate has been assessed with FEX (Gillies *et al*, 1998). The tryptophan fluorescence (excitation 295 nm, emission 350 nm) has been found to increase to approximately 10-fold in psoriatic lesions compared to age-matched control skin and to return to normal with treatment (Gillies *et al*, 2000). We have also found that the proliferation rate, as assessed by tryptophan fluorescence, from uninvolved skin surrounding active lesions yields substantially higher fluorescence signals than age-matched skin from normal subjects. Tyrosine fluorescence corresponding to epidermal inflammatory infiltrate (excitation 275 nm, emission 340 nm) has been found to decrease substantially with treatment.

Documentation of blood vessel morphology may be accomplished with epiluminescence video microscopy and an optical matching liquid. Water has proved an adequate medium in most cases because it minimizes the scattering from scale by hydration as well as the scattering from normal stratum corneum. Both vessel morphology and keratinocyte morphology may also be assessed *in vivo* with confocal microscopy. Confocal microscopy allows the characterization of additional microscopic features associated with psoriatic lesions such as keratinocyte morphology (Gonzalez *et al*, 1999).

Nonmelanoma skin cancer In the case of nonmelanoma skin cancer the parameters that have been assessed objectively include:

Proliferation
Cellular atypia
Erythema
Stratum corneum erosion
Matrix compromise

The erythema and stratum corneum erosion associated with nonmelanoma skin cancer may be documented using polarized light photography, erythema with the polarizing filters oriented perpendicular to each other and erosion with the polarizing filters oriented parallel to each other. FEX has been shown to provide measures for both the proliferation of epidermal keratinocytes and the compromise of the dermal matrix as the tumor grows (Kopf *et al*, 1995; Brancaleon *et al*, 2001). It has been shown that as the tumor grows the induced expression of matrix metalloproteinases results in compromise of the structural matrix. The fluorescence of collagenase digestible collagen cross-links has been shown to decrease in the tissue where the tumor has invaded the dermis and fluorescence imaging has been found to document the margins of the lesion. This collagen cross-link fluorescence is not altered when the lesions are confined entirely in the epidermis as in squamous cell carcinoma *in situ*. Another exception is found in morpheaform basal cell carcinoma where the lesional collagen fluorescence increases as the matrix is invaded by the tumor (data not published).

Scanning confocal microscopy has been shown to provide accurate documentation of keratinocyte morphology and atypia (Kopf *et al*, 1995; Busam *et al*, 2001; Rajadhyaksha *et al*, 2001). It has been used to evaluate the extent of tumors both *in vitro* in conjunction with Moes micrographic surgery and *in vivo*.

CONCLUSION

We have provided evidence that optical and computer technology is rapidly advancing, developing ever smaller and less expensive tools for aiding in clinical practice. Single point measurement instruments are now small, easily transportable to the bedside, and provide objective measures of a large number of molecular species in the skin *in vivo* noninvasively, thus providing objective measures of disease progression and response to treatment. Specialized imaging with small systems can address the documentation needs of the dermatologist for severity and extent of disease. Bench-top technologies show great promise for the near future, as instruments become smaller and less expensive to purchase and to operate. Judicious use of these instrumental modalities will help to move cutaneous disease assessment and diagnosis beyond subjective visual assessment.

REFERENCES

Andersen PH, Bjerring P: Noninvasive computerized analysis of skin chromophores *in vivo* by reflectance spectroscopy. *Photodermatol Photoimmunol Photomed* 7: 249–257, 1990

Anderson RR: Polarized light examination and photography of the skin. *Arch Dermatol* 127:1000–1005, 1991

Anderson RR, Parrish JA: The optics of human skin. *J Invest Dermatol* 77:13–19, 1981

Bissonnette R, Zeng H, McLean DI, Schreiber WE, Roscoe DL, Lui H: Psoriatic plaques exhibit red autofluorescence that is due to protoporphyrin IX. *J Invest Dermatol* 111:586–591, 1998

Bommannan D, Potts RO, Guy RH: Examination of stratum corneum barrier function *in vivo* by infrared spectroscopy. *J Invest Dermatol* 95:403–408, 1990

Brancaleon L, Lin G, Kollias N: The *in vivo* fluorescence of tryptophan moieties in human skin increases with UV exposure and is a marker for epidermal proliferation. *J Invest Dermatol* 113:977–982, 1999

Brancaleon L, Bamberg MP, Kollias N: Spectral differences between stratum corneum and sebaceous molecular components in the mid-IR. *Appl Spectroscopy* 54:1175–1182, 2000

Brancaleon L, Bamberg MP, Sakamaki T, Kollias N: Attenuated total reflection-Fourier transform infrared spectroscopy as a possible method to investigate biophysical parameters of stratum corneum *in vivo*. *J Invest Dermatol* 116: 380–386, 2001a

Brancaleon L, Durkin AJ, Tu JH, Menaker G, Fallon JD, Kollias N: *In vivo* fluorescence spectroscopy of nonmelanoma skin cancer. *Photochem Photobiol* 73: 178–183, 2001b

Busam KJ, Hester K, Charles C, *et al*: Detection of clinically amelanotic malignant melanoma and assessment of its margins by *in vivo* confocal scanning laser microscopy. *Arch Dermatol* 137:923–929, 2001

Bussau LJ, Vo LT, Delaney PM, Papworth GD, Barkla DH, King RG: Fibre optic confocal imaging (FOCI) of keratinocytes, blood vessels and nerves in hairless mouse skin *in vivo*. *J Anat* 192:187–194, 1998

Caspers PJ, Lucassen GW, Wolthuis R, Bruining HA, Puppels GJ: *In vitro* and *in vivo* Raman spectroscopy of human skin. *Biospectroscopy* 4 (Suppl.): S31–S39, 1998

Caspers PJ, Lucassen GW, Carter EA, Bruining HA, Puppels GJ: *In vivo* confocal Raman microspectroscopy of the skin: noninvasive determination of molecular concentration profiles. *J Invest Dermatol* 116:434–442, 2001

Corcuff P, Bertrand C, Leveque JL: Morphometry of human epidermis *in vivo* by real-time confocal microscopy. *Arch Dermatol Res* 285:475–481, 1993

Corcuff P, Chaussepied C, Madry G, Hadjur C: Skin optics revisited by *in vivo* confocal microscopy: melanin and sun exposure. *J Cosmet Sci* 52:91–102, 2001

Doukas AG, Soukos NS, Babusis S, Appa Y, Kollias N: Fluorescence excitation spectroscopy for the measurement of epidermal proliferation. *Photochem Photobiol* 74:96–102, 2001

Edwards EA, Duntley SQ: The pigments and color of living human skin. *Am J Anat* 65:1–33, 1939

Eun HC: Evaluation of skin blood flow by laser Doppler flowmetry. *Clin Dermatol* 13:337–347, 1995

Farkas DL, Becker D: Applications of spectral imaging: detection and analysis of human melanoma and its precursors. *Pigment Cell Res* 14:2–8, 2001

Farrell TJ, Patterson MS, Wilson B: A diffusion theory model of spatially resolved, steady-state diffuse reflectance for the noninvasive determination of tissue optical properties *in vivo*. *Med Phys* 19:879–888, 1992

Frushour BG, Koenig JL: Raman scattering of collagen, gelatin, and elastin. *Biopolymers* 14:379–391, 1975

Fulton JE: Utilizing the ultraviolet (UV detect) camera to enhance the appearance of photodamage and other skin conditions. *Dermatol Surg* 23:163–169, 1997

van Gemert MJ, Jacques SL, Sterenborg HJ, Star WM: Skin optics. *IEEE Trans Biomed Eng* 36:1146–1154, 1989

van Gemert MJ, Nelson JS, Milner TE, *et al*: Non-invasive determination of port wine stain anatomy and physiology for optimal laser treatment strategies. *Phys Med Biol* 42:937–950, 1997

Gillies R, Tian WD, Anderson RR, Drake LA, Kollias N: Noninvasive monitoring of treatment related changes in psoriatic plaques using fluorescence excitation and diffuse reflectance spectroscopy. In: Sevick-Muraca EM, Izatt JA Edinger MN, eds. *Trends in Optics and Photonics: Biomedical Optical Spectroscopy and Diagnosis*. Washington, DC: Optical Society of America, 1998: pp 113–115

Gillies R, Zonios G, Anderson RR, Kollias N: Fluorescence excitation spectroscopy provides information about human skin *in vivo*. *J Invest Dermatol* 115:704–707, 2000

Gniadecka M, Wulf HC, Nielsen OF, Christensen DH, Hercogova J: Distinctive molecular abnormalities in benign and malignant skin lesions: studies by Raman spectroscopy. *Photochem Photobiol* 66:418–423, 1997

Gniadecka M, Faurskov Nielsen O, Christensen DH, Wulf HC: Structure of water, proteins, and lipids in intact human skin, hair, and nail. *J Invest Dermatol* 110:393–398, 1998

Gonzalez S, Hegyi V, Baqer A, Sadiq I, Kollias N: Development of cutaneous tolerance to ultraviolet B during ultraviolet B phototherapy for psoriasis. *Photodermatol Photoimmunol Photomed* 12:73–78, 1996

Gonzalez S, Rajadhyaksha M, Anderson RR: Non-invasive (real-time) imaging of histologic margin of a proliferative skin lesion *in vivo*. *J Invest Dermatol* 111: 538–539, 1998

Gonzalez S, Rajadhyaksha M, Rubinstein G, Anderson RR: Characterization of psoriasis *in vivo* by reflectance confocal microscopy. *J Med* 30:337–356, 1999

Gonzalez S, Zonios G, Nguyen BC, Gillies R, Kollias N: Endogenous skin fluorescence is a good marker for objective evaluation of comedolysis. *J Invest Dermatol* 115:100–105, 2000

Hata TR, Scholz TA, Ermakov IV, *et al*: Non-invasive Raman spectroscopic detection of carotenoids in human skin. *J Invest Dermatol* 115:441–448, 2000

Hecht E, Zajac A: *Optics*, 4th edn. Reading, MA: Addison-Wesley Co, 1979

Hee MR, Izatt JA, Swanson EA, *et al*: Optical coherence tomography of the human retina. *Arch Ophthalmol* 113:325–332, 1995

Huzaira M, Rius F, Rajadhyaksha M, Anderson RR, Gonzalez S: Topographic variations in normal skin, as viewed by *in vivo* reflectance confocal microscopy. *J Invest Dermatol* 116:846–852, 2001

Jemec GB, Gniadecka M, Ulrich J: Ultrasound in dermatology. Part I. High frequency ultrasound. *Eur J Dermatol* 10:492–497, 2000

Knuttel A, Boehlau-Godau M: Spatially confined and temporally resolved refractive index and scattering evaluation in human skin performed with optical coherence tomography. *J Biomed Opt* 5:83–92, 2000

Kollias N: UVA melanogenesis – spectral observations. In Urbach F, ed. *Biological Responses to UVA Radiation*. Overland Park, KS: Valdenmar Publishers Co, 1992

Kollias N, Baqer A: An experimental study of the changes in pigmentation in human skin *in vivo* with visible and near infrared light. *Photochem Photobiol* 39:651–659, 1984

Kollias N, Baqer A: On the assessment of melanin in human skin *in vivo*. *Photochem Photobiol* 43:49–54, 1986

Kollias N, Baqer AH: Absorption mechanisms of human melanin in the visible, 400–720 nm. *J Invest Dermatol* 89:384–388, 1987

Kollias N, Baqer AH: Quantitative assessment of UV-induced pigmentation and erythema. *Photodermatol* 5:53–60, 1988

Kollias N, Baqer A, Sadiq I: Minimum erythema dose determination in individuals of skin type V and VI with diffuse reflectance spectroscopy. *Photodermatol Photoimmunol Photomed* 10:249–254, 1994

Kollias N, Gillies R, Muccini JA, Uyeyama RK, Phillips SB, Drake LA: A single parameter, oxygenated hemoglobin, can be used to quantify experimental irritant-induced inflammation. *J Invest Dermatol* 104:421–424, 1995

Kollias N, Gillies R, Cohen-Goihman C, *et al*: Fluorescence photography in the evaluation of hyperpigmentation in photodamaged skin. *J Am Acad Dermatol* 36(Part 1): 226–230, 1997

Kollias N, Gillies R, Moran M, Kochevar IE, Anderson RR: Endogenous skin fluorescence includes bands that may serve as quantitative markers of aging and photoaging. *J Invest Dermatol* 111:776–780, 1998

Kollias N, Stamatas GN, Youn JI: Suppression of UVB-induced cutaneous erythema by a previous UVB exposure. *Photochem Photobiol* 74:471–476, 2001

Kopf AW, Salopek TG, Slade J, Marghoob AA, Bart RS: Techniques of cutaneous examination for the detection of skin cancer. *Cancer* 75(Suppl.): 684–690, 1995

Leffell DJ, Stetz ML, Milstone LM, Deckelbaum LI: *In vivo* fluorescence of human skin. A potential marker of photoaging. *Arch Dermatol* 124:1514–1518, 1988

Lohmann W, Paul E: *In situ* detection of melanomas by fluorescence measurements. *Naturwissenschaften* 75:201–202, 1988

Lohmann W, Schill WB, Bucher D, *et al*: Elastosis and cancer. *Z Naturforsch [C]* 49:223–229, 1994

Lucassen GW, van Veen GNA, Jansen, JAJ: Band analysis of hydrated human skin stratum corneum attenuated total reflectance Fourier transform infrared spectra *in vivo*. *J Biomed Opt* 3:267–280, 1998

Lucchina LC, Kollias N, Gillies R, *et al*: Fluorescence photography in the evaluation of acne. *J Am Acad Dermatol* 35:58–63, 1996

Mak VH, Potts RO, Guy RH: Percutaneous penetration enhancement *in vivo* measured by attenuated total reflectance infrared spectroscopy. *Pharm Res* 7: 835–841, 1990

Marchesini R, Tomatis S, Bartoli C, *et al*: *In vivo* spectrophotometric evaluation of neoplastic and non-neoplastic skin pigmented lesions. III. CCD camera-based reflectance imaging. *Photochem Photobiol* 62:151–154, 1995

Masters BR, Gonnord G, Corcuff P: Three-dimensional microscopic biopsy of *in vivo* human skin: a new technique based on a flexible confocal microscope. *J Microsc* 185(Part 3): 329–338, 1997a

Masters BR, So PT, Gratton E: Multiphoton excitation fluorescence microscopy and spectroscopy of *in vivo* human skin. *Biophys J* 72:2405–2412, 1997b

Masters BR, So PT, Gratton E: Multiphoton excitation microscopy of *in vivo* human skin. Functional and morphological optical biopsy based on three-dimensional imaging, lifetime measurements and fluorescence spectroscopy. *Ann N Y Acad Sci* 838:58–67, 1998

Masters BR, So PT, Kim KH, Buehler C, Gratton E: Multiphoton excitation microscopy, confocal microscopy, and spectroscopy of living cells and tissues; functional metabolic imaging of human skin *in vivo*. *Methods Enzymol* 307:513–536, 1999

McIntosh LM, Jackson M, Mantsch HH, Stranc MF, Pilavdzic D, Crowson AN: Infrared spectra of basal cell carcinomas are distinct from non-tumor-bearing skin components. *J Invest Dermatol* 112:951–956, 1999

McIntosh LM, Summers R, Jackson M, *et al*: Towards non-invasive screening of skin lesions by near-infrared spectroscopy. *J Invest Dermatol* 116:175–181, 2001

Muccini JA, Kollias N, Phillips SB, *et al*: Polarized light photography in the evaluation of photoaging. *J Am Acad Dermatol* 33(Part 1): 765–769, 1995

Mustakallio KK, Korhonen P: Monochromatic ultraviolet-photography in dermatology. *J Invest Dermatol* 47:351–356, 1966

Na R, Stender IM, Henriksen M, Wulf HC: Autofluorescence of human skin is age-related after correction for skin pigmentation and redness. *J Invest Dermatol* 116:536–540, 2001

Oberg PA: Laser-Doppler flowmetry. *Crit Rev Biomed Eng* 18:125–163, 1990

Pagnoni A, Kligman AM, Kollias N, Goldberg S, Stoudemayer T: Digital fluorescence photography can assess the suppressive effect of benzoyl peroxide on *Propionibacterium acnes*. *J Am Acad Dermatol* 41(Part 1): 710–716, 1999

Phillips SB, Kollias N, Gillies R, Muccini JA, Drake LA: Polarized light photography enhances visualization of inflammatory lesions of acne vulgaris. *J Am Acad Dermatol* 37:948–952, 1997

Pouliot R, Germain L, Auger FA, Tremblay N, Juhasz J: Physical characterization of the stratum corneum of an *in vitro* human skin equivalent produced by tissue engineering and its comparison with normal human skin by ATR-FTIR spectroscopy and thermal analysis (DSC). *Biochim Biophys Acta* 1439:341–352, 1999

Rajadhyaksha M, Grossman M, Esterowitz D, Webb RH, Anderson RR: *In vivo* confocal scanning laser microscopy of human skin: melanin provides strong contrast. *J Invest Dermatol* 104:946–952, 1995

Rajadhyaksha M, Gonzalez S, Zavislan JM, Anderson RR, Webb RH: *In vivo* confocal scanning laser microscopy of human skin II. Advances in instrumentation and comparison with histology. *J Invest Dermatol* 113:293–303, 1999

Rajadhyaksha M, Menaker G, Flotte T, Dwyer PJ, Gonzalez S: Confocal examination of nonmelanoma cancers in thick skin excisions to potentially guide Mohs micrographic surgery without frozen histopathology. *J Invest Dermatol* 117:1137–1143, 2001

Richards-Kortum R, Sevick-Muraca E: Quantitative optical spectroscopy for tissue diagnosis. *Annu Rev Phys Chem* 47:555–606, 1996

Savolainen L, Kontinen J, Roning J, Oikarinen A: Application of machine vision to assess involved surface in patients with psoriasis. *Br J Dermatol* 137:395–400, 1997

Schallreuter KU, Moore J, Wood JM, *et al*: *In vivo* and *in vitro* evidence for hydrogen peroxide (H_2O_2) accumulation in the epidermis of patients with vitiligo and its successful removal by a UVB-activated pseudocatalase. *J Invest Dermatol Symp Proc The* 4:91–96, 1999

Tanaka M, Gaskell S, Edwards C, Marks R: Simple horizontal averaging programme enables shade correction for image analysis in psoriasis. *Clin Exp Dermatol* 25:323–326, 2000

Tian WD, Gillies R, Brancaleon L, Kollias N: Aging and effects of ultraviolet A exposure may be quantified by fluorescence excitation spectroscopy *in vivo*. *J Invest Dermatol* 116:840–845, 2001

Ulrich J, Voit C: Ultrasound in dermatology Part II. Ultrasound of regional lymph node basins and subcutaneous tumours. *Eur J Dermatol* 11:73–79, 2001

Unholzer A, Korting HC: High-frequency ultrasound in the evaluation of pharmacological effects on the skin. *Skin Pharmacol Appl Skin Physiol* 15:71–84, 2002

Vitkin IA, Woolsey J, Wilson BC, Anderson RR: Optical and thermal characterization of natural (Sepia officinalis) melanin. *Photochem Photobiol* 59:455–462, 1994

Vo LT, Papworth GD, Delaney PM, Barkla DH, King RG: A study of vascular response to thermal injury on hairless mice by fibre optic confocal imaging, laser doppler flowmetry and conventional histology. *Burns* 24:319–324, 1998

Vo LT, Anikijenko P, McLaren WJ, Delaney PM, Barkla DH, King RG: Autofluorescence of skin burns detected by fiber-optic confocal imaging: evidence that cool water treatment limits progressive thermal damage in anesthetized hairless mice. *J Trauma* 51:98–104, 2001

Wan S, Anderson RR, Parrish JA: Analytical modeling for the optical properties of the skin with in vitro and *in vivo* applications. *Photochem Photobiol* 34:493–499, 1981

Welzel J, Lankenau E, Birngruber R, Engelhardt R: Optical coherence tomography of the human skin. *J Am Acad Dermatol* 37:958–963, 1997

White PJ, Fogarty RD, Liepe IJ, Delaney PM, Werther GA, Wraight CJ: Live confocal microscopy of oligonucleotide uptake by keratinocytes in human skin grafts on nude mice. *J Invest Dermatol* 112:887–892, 1999

Wohlrab J, Vollmann A, Wartewig S, Marsch WC, Neubert R: Noninvasive characterization of human stratum corneum of undiseased skin of patients with atopic dermatitis and psoriasis as studied by Fourier transform Raman spectroscopy. *Biopolymers* 62:141–146, 2001

Young AR: Chromophores in human skin. *Phys Med Biol* 42:789–802, 1997

Zeng H, MacAulay C, McLean DI, Palcic B: Spectroscopic and microscopic characteristics of human skin autofluorescence emission. *Photochem Photobiol* 61: 639–645, 1995

Zeng H, MacAulay C, McLean DI, Palcic B, Lui H: The dynamics of laser-induced changes in human skin autofluorescence–experimental measurements and theoretical modeling. *Photochem Photobiol* 68:227–236, 1998

Zonios G, Bykowski J, Kollias N: Skin melanin, hemoglobin, and light scattering properties can be quantitatively assessed *in vivo* using diffuse reflectance spectroscopy. *J Invest Dermatol Press* 117:1452–1457, 2001